

A Dual-Porosity Model for Simulating the Preferential Movement of Water and Solutes in Structured Porous Media

H. H. GERKE¹ AND M. T. VAN GENUCHTEN

U.S. Salinity Laboratory, USDA, ARS, Riverside, California

A one-dimensional dual-porosity model has been developed for the purpose of studying variably saturated water flow and solute transport in structured soils or fractured rocks. The model involves two overlaying continua at the macroscopic level: a macropore or fracture pore system and a less permeable matrix pore system. Water in both pore systems is assumed to be mobile. Variably saturated water flow in the matrix as well as in the fracture pore system is described with the Richards' equation, and solute transport is described with the convection-dispersion equation. Transfer of water and solutes between the two pore regions is simulated by means of first-order rate equations. The mass transfer term for solute transport includes both convective and diffusive components. The formulation leads to two coupled systems of nonlinear partial differential equations which were solved numerically using the Galerkin finite element method. Simulation results demonstrate the complicated nature of solute leaching in structured, unsaturated porous media during transient water flow. Sensitivity studies show the importance of having accurate estimates of the hydraulic conductivity near the surface of soil aggregates or rock matrix blocks. The proposed model is capable of simulating preferential flow situations using parameters which can be related to physical and chemical properties of the medium.

INTRODUCTION

Porous media often exhibit a variety of heterogeneities, such as fractures, fissures, cracks, and macropores or inter-aggregate pores, and sometimes also show dynamic instabilities of the wetting front during infiltration. These microscopic structures or processes affect water and solute movement at the macroscopic level by creating nonuniform flow fields with widely different velocities. Such phenomena are often referred to as preferential flow [Beven, 1991]. They have been extensively studied for exploitation of fissured groundwater and petroleum reservoirs [Barenblatt *et al.*, 1960; Warren and Root, 1963]. Similar problems are reported also for flow and transport in unsaturated fractured rocks [Evans and Nicholson, 1987; Pruess and Wang, 1987; Wang, 1991], for macroporous or structured field soils [Beven and Germann, 1982; Nielsen *et al.*, 1986; Steenhuis and Parlange, 1991], and even for seemingly homogeneous coarse-textured soils [Hill and Parlange, 1972; Glass *et al.*, 1989; Kung, 1990a, b; Baker and Hillel, 1991]. Preferential flow leads to an apparent nonequilibrium situation with respect to the pressure head or the solute concentration, or both [Brusseu and Rao, 1990; Wang, 1991], and severely limits our ability to predict flow and transport processes in undisturbed media.

Flow and transport in structured porous media are frequently described using double-porosity (or dual) models. Such an approach assumes that the medium consists of two regions, one associated with the macropore or fracture network and the other with a less permeable pore system of soil aggregates or rock matrix blocks. Double-porosity models may be obtained using volume averaging techniques [Long *et al.*, 1982; Moench, 1984] or, alternatively, with the method of homogenization [Arbogast *et al.*, 1990; Hornung

and Showalter, 1990] which assumes that the medium is periodic at a smaller scale. Both methods yield equivalent results at the macroscopic scale [Wheatcraft and Cushman, 1991] for single-phase flow and diffusion-type models. Dual-porosity models assume that both water flow and solute transport can be described by two equations which are coupled using a term characterizing the exchange of fluid or solutes between the two pore regions. Special cases include (1) compartment or first-order rate models in which flow or transport between the matrix blocks is assumed to be negligible, (2) fissured medium models which, in addition, assume the storage term for the fissures to be negligible, and (3) microstructure models which consider the dynamics of flow and transport at the local scale of individual matrix blocks [Hornung and Showalter, 1990].

A large number of models using the two-domain or multi-domain concept have been used to describe water flow and/or solute transport in macroporous soils [e.g., Edwards *et al.*, 1979; Hoogmoed and Bouma, 1980; Beven and Germann, 1981; Davidson, 1985; Bruggeman and Mostaghimi, 1991], unsaturated fractured rocks [Berkowitz *et al.*, 1988; Dudley *et al.*, 1988], and fissured groundwater systems [Barenblatt *et al.*, 1960; Duguid and Lee, 1977; Bibby, 1981]. Compartment models have been suggested for flow in fractured reservoirs and solute transport in structured soils [Warren and Root, 1963; Coats and Smith, 1964; van Genuchten and Wierenga, 1976]. Several authors also assumed a specific geometry of the macropores or fractures for water flow [Wang and Narasimhan, 1985; Pruess *et al.*, 1990a] or solute transport [Neretnieks and Rasmuson, 1984; van Genuchten and Dalton, 1986]. Most of these models are limited to conditions of water saturation or steady state flow, to water flow only, or to conditions for which flow or storage in one pore system can be neglected. Others have considerably simplified the representation of the fracture and matrix block geometry. Unfortunately, well-defined geometry-based models are difficult to apply to actual field situations since they require an excessive amount of information about the geometry of the structural units; this type of information

¹Now at Destedt, Germany.

This paper is not subject to U.S. copyright. Published in 1993 by the American Geophysical Union.

Paper number 92WR02339.

is seldom available. Also, water flow in most undisturbed soils has been observed to occur in the macropores as well as in the soil matrix [e.g., White, 1985; Hornberger *et al.*, 1990]. Indirect evidence of water flow through both the matrix pores and the fracture network was obtained by Gvirtzman *et al.* [1988, 1990] from natural tritium concentration profiles in calcareous sandstone, as well as in sandy and clayey eolian loess sediments.

Skopp *et al.* [1981] proposed an extension of the compartment model approach to situations where water in both pore systems is mobile. While conceptually attractive, their approach is still limited to steady state flow, while the approximate analytical solution is valid only for relatively small interactions between the two regions. Solute transport will become much more complicated during transient flow because of the influence of such factors as the soil surface boundary condition [Bond and Wierenga, 1990], the water application rate [White *et al.*, 1986b], and the initial condition [White *et al.*, 1986a; Kluitenberg and Horton, 1990]. Variably saturated transient water flow in both pore systems was considered by Yeh and Luxmoore [1982], who simulate solute transport in two coupled, overlapping macropore-mesopore media. Double-porosity models for variably saturated water flow and solute transport in fractured rocks were also proposed by Dykhuizen [1987] and Dudley *et al.* [1988]. These two studies applied the Richards' equation for water flow and the convection-dispersion equation for solute transport to both pore regions. However, the generality of the water flow model was reduced considerably by invoking the assumption that the pressure head will equilibrate instantaneously between the fracture and matrix regions. This assumption leads to a single flow equation involving a composite set of unsaturated hydraulic functions for the structured medium as a whole [Dykhuizen, 1987; Peters and Klavetter, 1988; Pruess *et al.*, 1990b].

Steenhuis *et al.* [1990] recently proposed an approximate numerical model for preferential flow which incorporates several instead of only two pore water velocity regions. The multiple domains were obtained by grouping pore sizes using information derived from piecewise linear approximations of the unsaturated hydraulic conductivity function. Convective solute transport in each pore group was simulated using a mixing cell procedure, while also allowing for interactions between various pore domains. In yet another formulation, Workman and Skaggs [1990] simulated the ponded infiltration of water into a soil containing a single representative cylindrical macropore. Macropore flow was described with the Hagen-Poiseuille' law, while infiltration from the macropores into the matrix was modeled by means of an empirical term containing the pressure head gradient as the driving force. Jarvis *et al.* [1991a, b] proposed a dual-porosity model which also included swelling and shrinking of a clay soil. Water flow in the macropore domain was modeled using the unit hydraulic gradient assumption, while solute transport in this domain was assumed to occur by convection only. Water flow between the two regions was described with a quasi-empirical equation using relative saturation as a driving force, while solute exchange occurred by both convective and diffusive transport. In other approaches, vertical flow of water along the macropore walls was described with a kinematic wave equation [Beven, 1981, 1982; Germann and Beven, 1985], or a boundary layer flow theory assuming viscous flow [Germann, 1990]. Chen and Wagenet [1992a],

on the other hand, used the Chezy-Manning equation to describe the presumed turbulent flow process in the macropore domain, while employing Philip's infiltration equation to describe mass exchange between the two regions. These same authors [Chen and Wagenet, 1992b] subsequently used filter theory to simplify the Richards' and convection-dispersion equations, thereby facilitating the use of analytical solutions for flow and transport in the matrix and macropore domains.

The numerical dual-porosity model proposed in this paper assumes that the Richards' equation for transient water flow and the convection-dispersion equation for solute transport can be applied to both pore systems. Similar to the two-region compartment model, water and solute mass transfer between the two pore systems will be described with quasi-empirical first-order rate equations. The double-porosity concept will be studied by means of simulation examples involving transient water flow and solute transport in variably saturated structured porous media. The sensitivity of model results to selected flow parameters will be investigated, and the utility of the model for practical applications will be discussed.

CONCEPTUAL MODEL

Central to the dual-porosity approach is the assumption that the medium can be separated into two distinct pore systems, both of which are treated as homogeneous media with separate hydraulic and solute transport properties. The dual-porosity medium is considered to be a superposition of these two systems over the same volume [Dykhuizen, 1987]. The two pore systems interact by exchanging water and solutes in response to pressure head and concentration gradients. Hence macroscopically, the porous medium at any point in time and space is characterized by two flow velocities, two pressure heads, two water contents, and two solute concentrations.

Microscopically, a structured porous medium consists of soil aggregates or rock matrix blocks (shaded irregular blocks in Figure 1) surrounded by interaggregate pores or fractures (dotted areas in Figure 1) which form a more or less continuous network. While consisting mainly of the larger pores, the soil macropore network may also include mesopores and micropores in the immediate vicinity of the macropores [Wilson and Luxmoore, 1988; Jardine *et al.*, 1990; Luxmoore *et al.*, 1990], as well as some mineral or organic particles along the macropore walls [Schoeneberger and Amoozegar, 1990]. The fracture network in rocks may form a continuum consisting of different pore sizes [Long *et al.*, 1982; Berkowitz *et al.*, 1988]; it may be rough walled or contain some filling material [Tsang and Tsang, 1987]. Similarly, the matrix may contain some discontinuous (blind) macropores or fractures which do not affect the hydraulic conductivity. We will further use the subscript *f* to denote the macropore or interaggregate pore system in a soil, or the fracture network in a fractured rock formation, and the subscript *m* for the soil or rock matrix.

A dual-porosity type structured medium is hypothesized here to involve two water retention functions (Figure 2a), one for the matrix and one for the fracture pore system, but three hydraulic conductivities functions: $K_f(h_f)$, $K_m(h_m)$ and $K_a(\bar{h})$ (Figure 2b). We will use $K_f(h_f)$ for the hydraulic conductivity of the fracture network (defined here per unit

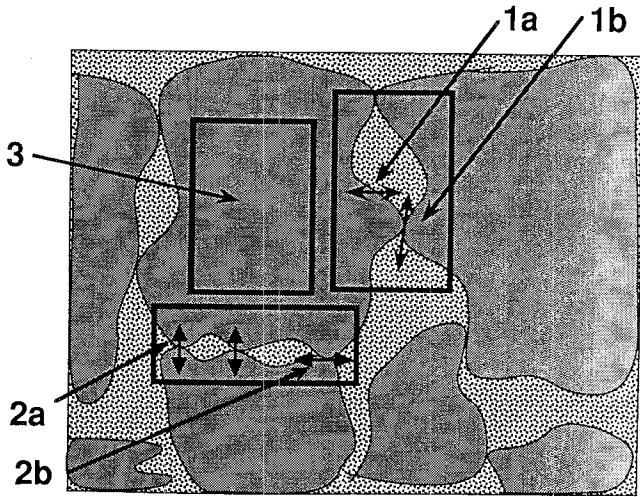


Fig. 1. Schematic picture of a vertical cross-section of a structured porous medium at the microscopic level. The shaded areas indicate soil aggregates or rock matrix blocks, whereas the dotted areas portray the macropore, interaggregate, or fracture pore network. The framed areas display regions with water and solute movement through the surface of an aggregate (1a), through the fracture pore network (1b), between aggregates (2a), between continuous and stagnant fracture pore space (2b), and inside an aggregate (3).

total volume $V_{t,f}$ of the fracture pore system) as a function of the fracture pressure head h_f . The function $K_f(h_f)$ depends, among other things, on factors characterizing the structure of the fracture pore space (area 1b in Figure 1), such as pore size, geometry, continuity, wall roughness, or presence of possible fracture fillings. Similarly, $K_m(h_m)$ is the hydraulic

conductivity of the matrix system (defined per unit total volume $V_{t,m}$ of the matrix pore system) as a function of the matrix pressure head h_m . While determined primarily by the hydraulic properties of single matrix blocks (area 3 in Figure 1), $K_m(h_m)$ depends also on the continuity of the matrix pore system and on the area of water-filled menisci around contact points between adjoining matrix blocks (area 2a in Figure 1) during unsaturated flow. Finally, $K_a(\bar{h})$ is the effective hydraulic conductivity to be used in equations describing the exchange of water between the two pore systems (areas 1a in Figure 1). $K_a(\bar{h})$, defined here per unit total volume V_t of the medium, is evaluated at a pressure head \bar{h} which is some average of the pressure heads of the matrix and fracture pore systems. As a first approximation, K_a is probably best represented by the conductivity function of the matrix. However, the local bulk density of a soil aggregate is often higher near its surface than in the aggregate center (e.g., *Gunzelmann [1990]*, who also obtained measurements of K_a on single soil aggregates) because of deposits of organic matter, fine-texture mineral particles, or various oxides and hydroxides along macropore walls. Similarly, rock formations may exhibit fracture skins [*Moench, 1984*], fracture wall, or matrix block coatings [*Wang and Narasimhan, 1985; Pruess and Wang, 1987; Thoma et al., 1992*] involving deposits of clay, calcite, zeolite, or silicates. On the other hand, some fractured rocks may also have lower local bulk densities (and hence higher conductivities) near a fracture face, as compared to the matrix interior, because of weathering or other physicochemical processes. Another complication in accurately defining $K_a(\bar{h})$ is that the exchange of water and solutes between the two pore systems may be restricted to only a small portion of the total interface area [*Hoogmoed and Bouma, 1980*], e.g., because of prefer-

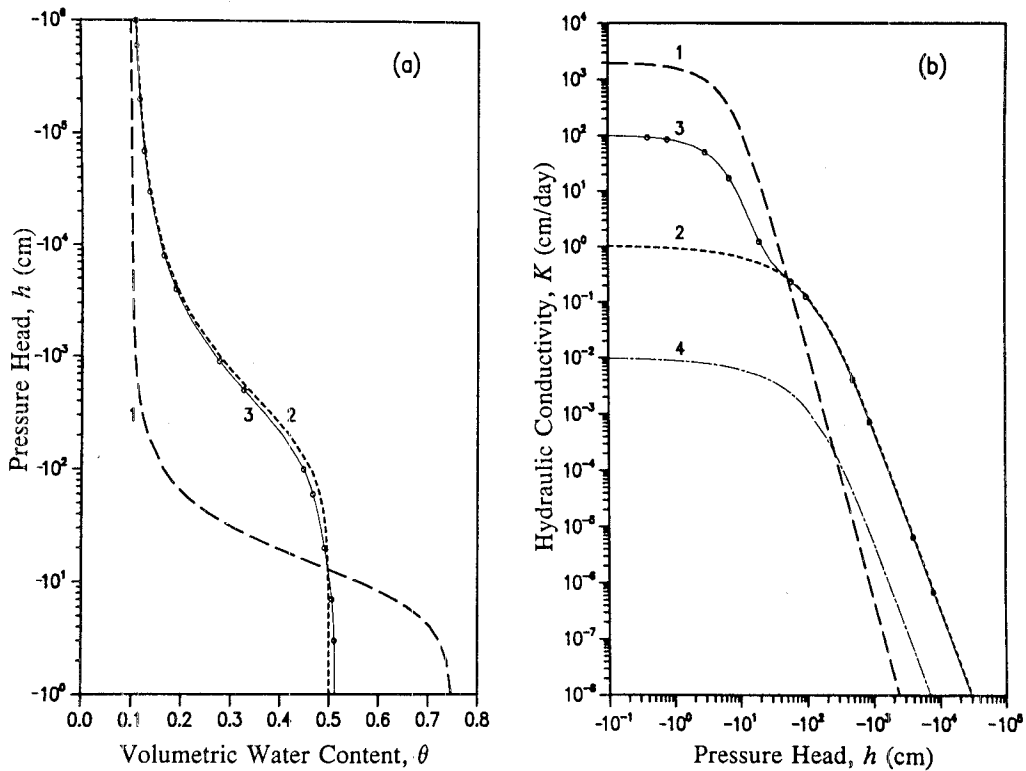


Fig. 2. Hydraulic properties of a dual-porosity medium: (a) Retention and (b) hydraulic conductivity functions of fracture (1) and matrix (2) pore systems, of the total porous medium (3), and of the exchange term (4).

ential flow within the macropores and/or the possible hydrophobic nature of some of the deposits on the macropore walls. Estimates of the K_f and K_m functions may be obtained by assuming that K_f is primarily the weighted bulk conductivity function in the wet range and K_m that in the dry range. Figure 2 gives a schematic representation of the hydraulic properties of a dual-porosity medium; also included are the properties of an equivalent composite medium assuming a single porosity.

Let us define the porosity ε of a structured medium as the volume V_p of pores per unit volume of the medium V_t , i.e., $\varepsilon = V_p/V_t$. Similarly, $\varepsilon_f = V_{p,f}/V_{t,f}$ and $\varepsilon_m = V_{p,m}/V_{t,m}$ are the (local) porosities of the fracture and matrix pore systems, respectively. Notice that $V_p = V_{p,f} + V_{p,m}$ and $V_t = V_{t,f} + V_{t,m}$. The three porosities are related by

$$\varepsilon = w_f \varepsilon_f + (1 - w_f) \varepsilon_m \quad (1)$$

in which w_f is a volumetric weighting factor given by

$$w_f = V_{t,f}/V_t \quad (2)$$

The (local) volumetric water constant of the fracture, θ_f , and matrix, θ_m , ($L^3 L^{-3}$) pore systems are defined as

$$\theta_f = V_{w,f}/V_{t,f}; \quad \theta_m = V_{w,m}/V_{t,m} \quad (3)$$

where $V_{w,f}$ and $V_{w,m}$ are the volumes of water (L^3) in the fracture and matrix pore systems, respectively. The water content of the bulk soil, $\theta = V_w/V_t$, is then given by

$$\theta = w_f \theta_f + (1 - w_f) \theta_m \quad (4)$$

The water flux densities q_f and q_m ($L T^{-1}$) for the two pore systems are

$$q_f = Q_f/A_f; \quad q_m = Q_m/A_m \quad (5)$$

where Q_f and Q_m are the volumes of water flowing per unit time through unit areas A_f and A_m of the fracture and matrix regions, respectively. The fluid flux density of the bulk soil at any given depth is

$$q = \frac{Q_f + Q_m}{A_f + A_m} \quad (6)$$

where $A_f = w_f A$ and $A_m = (1 - w_f)A$ in which A is the unit area of bulk soil perpendicular to the flow direction. We assume here that volumetric weighting as expressed by (2) is the same as areal weighting, i.e., $w_f = V_{t,f}/V_t = A_f/A$. Equation (6) can also be expressed in the form

$$q = w_f q_f + (1 - w_f) q_m \quad (7)$$

which shows that q represents the area-weighted fluid flux density. The pore water velocities v_f and v_m in the fracture and matrix regions are defined as

$$v_f = \frac{q_f}{\varepsilon_f S_{w,f}} = \frac{q_f}{\theta_f}; \quad v_m = \frac{q_m}{\varepsilon_m S_{w,m}} = \frac{q_m}{\theta_m} \quad (8)$$

where $S_{w,f}$ and $S_{w,m}$ represent the degrees of fluid saturation in the two pore systems. The average pore water velocity $v = q/\theta$ in the bulk soil follows immediately from (4) and (7).

An expression for the average bulk soil hydraulic conductivity K can be derived by substituting Darcy's flux law into (7) yielding

$$K \left(\frac{\partial h}{\partial z} - 1 \right) = w_f K_f \left(\frac{\partial h_f}{\partial z} - 1 \right) + (1 - w_f) K_m \left(\frac{\partial h_m}{\partial z} - 1 \right) \quad (9)$$

where h is the pressure head (L) associated with the bulk soil and z is the soil depth (L) which is defined positive downward. Equation (9) reduces to

$$K = w_f K_f + (1 - w_f) K_m \quad (10)$$

if $h = h_m = h_f$, which is the equilibrium assumption used by Peters and Klavetter [1988], among others. Equation (10) also holds during steady state unsaturated flow when the pressure head gradient $\partial h/\partial z$ in both pore systems becomes zero or when the system is completely saturated ($K = K_s$). Finally, a sink term for root water extraction from the bulk soil may be defined as

$$S = w_f S_f + (1 - w_f) S_m \quad (11)$$

which represents the volumetric average of the root water extraction terms of the two pore systems.

GOVERNING EQUATIONS

Darcy-type water flow is considered in both the fracture and matrix pore system, while the transfer of water and solutes between the two pore systems is described macroscopically using a first-order coupling term. We further assume that the densities of the fluid and solid phases are constant, ignore the effects of swelling and shrinking, assume no hysteresis in the hydraulic properties, and consider the effects of temperature, air pressure, and solute concentration on water flow to be negligible. One-dimensional vertical water flow in the fracture and matrix pore systems of a dual-porosity medium is then described by the following equations:

$$C_f \frac{\partial h_f}{\partial t} = \frac{\partial}{\partial z} \left(K_f \frac{\partial h_f}{\partial z} - K_f \right) - \frac{\Gamma_w}{w_f} - S_f \quad (12a)$$

$$C_m \frac{\partial h_m}{\partial t} = \frac{\partial}{\partial z} \left(K_m \frac{\partial h_m}{\partial z} - K_m \right) + \frac{\Gamma_w}{1 - w_f} - S_m \quad (12b)$$

respectively, where t is time, Γ_w is the space- and time-dependent exchange term (T^{-1}) describing the transfer of water (subscript w) between the two pore systems, $S(T^{-1})$ is a sink term to account for root water extraction, and $C(L^{-1})$ is the specific soil water capacity given by

$$C = S_w S_s + \varepsilon \frac{\partial S_w}{\partial h} \quad (13)$$

in which S_s is the specific storage coefficient (L^{-1}) and S_w the degree of fluid saturation. The soil water capacity during unsaturated conditions is closely approximated by the slope $d\theta/dh$ of the soil water retention function $\theta(h)$.

If $\Gamma_w > 0$ in (12a and 12b), water transfer is directed from the fracture system into the matrix. At any depth z , the transfer term Γ_w is assumed to be proportional to the difference in pressure head between the fracture and matrix pore system as follows:

$$\Gamma_w = \alpha_w (h_f - h_m) \quad (14)$$

where α_w is a first-order transfer coefficient for water ($L^{-1} T^{-1}$) (subscript w) defined as

$$\alpha_w = \alpha_w^* K_a \quad (15)$$

with

$$\alpha_w^* = \frac{\beta}{a^2} \gamma_w \quad (16)$$

where β is a factor depending on the geometry of the aggregates, a represents the distance (L) from the center of a fictitious matrix block to the fracture boundary, and γ_w is an empirical coefficient. Equation (16) was derived by comparing Laplace transforms of (15) with those of the linearized horizontal flow equation assuming a variety of aggregate geometries. We refer to Gerke and van Genuchten [1993] for a detailed discussion and evaluation of the water transfer term, including the manner in which the hydraulic conductivity K_a is evaluated as a function of the "average" pressure head, \bar{h} , at the interface between the two regions. The coefficient γ_w was found to be 0.4, more or less independent of the aggregate geometry and the applied initial pressure head conditions. As shown in previous literature on solute transport in dual-porosity (mobile-immobile) systems [e.g., Bolt, 1979; van Genuchten and Dalton, 1986], the geometry factor β equals 3 for rectangular slabs and 15 for spheres.

Similar to that for water flow, solute transport with linear adsorption and first-order decay in a dual-porosity medium is described by a coupled set of convection-dispersion equations:

$$\frac{\partial}{\partial t} (\theta_f R_f c_f) = \frac{\partial}{\partial z} \left(\theta_f D_f \frac{\partial c_f}{\partial z} - q_f c_f \right) - \theta_f \mu_f c_f - \frac{\Gamma_s}{w_f} \quad (17a)$$

$$\frac{\partial}{\partial t} (\theta_m R_m c_m) = \frac{\partial}{\partial z} \left(\theta_m D_m \frac{\partial c_m}{\partial z} - q_m c_m \right) - \theta_m \mu_m c_m + \frac{\Gamma_s}{1 - w_f} \quad (17b)$$

where the subscripts f and m refer to the fracture and matrix pore regions, respectively; c is the solute concentration ($M L^{-3}$), D is the dispersion coefficient ($L^2 T^{-1}$), μ is a first-order decay coefficient (T^{-1}), Γ_s is the solute (subscript s) mass transfer term ($M L^{-3} T^{-1}$), and R is the dimensionless retardation factor given as

$$R = 1 + \frac{\rho_b k}{\theta} \quad (18)$$

in which ρ_b is the bulk density ($M L^{-3}$) and k an adsorption coefficient ($M^{-1} L^3$). As before for water flow, all variables in (17a and 17b) are defined relative to the partial volume of each pore system. The only exception is the exchange term Γ_s , which is defined as the mass of solutes per unit volume of bulk soil per unit time. Both convective transport and diffusion/dispersion are hypothesized to contribute to Γ_s as follows:

$$\Gamma_s = (1 - d)\Gamma_w \phi_f c_f + d\Gamma_w \phi_m c_m + \alpha_s (1 - w_f) \theta_m (c_f - c_m) \quad (19)$$

where

$$d = 0.5 \left(1 - \frac{\Gamma_w}{|\Gamma_w|} \right), \quad \Gamma_w \neq 0 \quad (20)$$

$$\phi_f = w_f \frac{\theta_f}{\theta}; \quad \phi_m = (1 - w_f) \frac{\theta_m}{\theta} \quad (21)$$

in which Γ_w is the exchange term for water (T^{-1}) as defined previously, d is a dimensionless coefficient which determines the direction of flow between the two pore systems, ϕ_f and ϕ_m are dimensionless coefficients (21) relating the solute concentrations of the fracture and matrix pore system to the unit solute mass of the bulk soil, and α_s is the solute transfer coefficient (T^{-1}) given by

$$\alpha_s = \frac{\beta}{a^2} D_a \quad (22)$$

where D_a is the effective ionic or molecular diffusion coefficient ($L^2 T^{-1}$) of the matrix block near the interface. The diffusion coefficient D_a is equivalent to K_a in the water transfer term given by (15) and (16). Notice that the first two terms on the right-hand side of (19) define the convective contribution to μ_w , while the third term gives the diffusion contribution to the exchange term. The product $(1 - w_f)\theta_m$ in the third term specifies the volume of water in the matrix pore system per unit bulk volume; this product is needed to relate the amount of solute diffusing into or out of the matrix to the bulk volume. Equation (22) is the same as in previous two-region (mobile-immobile) studies for solute transport assuming no flow in the soil matrix pore system [van Genuchten and Dalton, 1986].

Equations (12a), (12b), (17a) and (17b) were solved subject to the usual initial and boundary conditions. The initial conditions (subscript i) in the fracture and matrix pore systems may be given in terms of the pressure head ($h_{f,i}(z)$, $h_{m,i}(z)$) or water content ($\theta_{f,i}(z)$, $\theta_{m,i}(z)$), and the solute concentration ($c_{f,i}(z)$, $c_{m,i}(z)$). The standard boundary conditions for water flow involve prescribed pressure heads ($h_{f,0}(t)$, $h_{m,0}(t)$ and $h_{f,l}(t)$, $h_{m,l}(t)$) or prescribed fluxes ($q_{f,0}(t)$, $q_{m,0}(t)$ and $q_{f,l}(t)$, $q_{m,l}(t)$) at the upper ($z = 0$) and lower ($z = l$) boundaries of the one-dimensional system. In addition, a free-draining profile may be imposed by assuming zero pressure head gradients at the lower boundary. For solute transport, the standard boundary conditions at $z = 0$ involve prescribed first-type ($c_{m,0}(t)$, $c_{f,0}(t)$) or third-type boundary conditions, where $c_0(t)$ is the concentration of the infiltrating water. At $z = l$ a zero-gradient boundary condition may be imposed during periods of drainage. During upward flow from a groundwater table, either a first- or third-type condition may be applied using $c_i(t)$ as the solute concentration of the incoming water.

The standard boundary conditions for water flow at the soil surface ($z = 0$) need modification when the applied surface flux, $q_{m,0}$, resulting from rainfall or irrigation, exceeds the infiltration capacity of the matrix pore system, i.e.,

$$q_{m,0}(t) > \left(-K_m \frac{\partial h_m}{\partial z} + K_m \right) \Big|_{z=0} \quad (23)$$

but remains less than the combined infiltration capacity of the fracture plus matrix pore systems. In that case, a zero or

TABLE 1. Hydraulic Parameters Used in the Simulations

	θ_r	θ_s	α , cm ⁻¹	n	l	K_s , cm/d	w	S_s , cm ⁻¹
Fracture	0.0	0.5	0.1	2.0	0.5	2000.0	0.05	10 ⁻⁷
Matrix	0.10526	0.5	0.005	1.5	0.5	1.0526	0.95	10 ⁻⁷
Exchange term	0.005	1.5	0.5	0.01

small positive pressure head $h_{m,0}^*(t)$ will develop at the surface of the matrix pore system, and the surface boundary condition for the soil matrix becomes

$$h_m(0, t) = h_{m,0}^*(t) \quad (24)$$

The flux $q_m^*(0, t)$ must subsequently be recalculated from condition (24) using the numerical solution, while the boundary flux $q_{f,0}^*(t)$ into the fracture system must be adjusted iteratively with the help of (7) during the numerical solution process, i.e.,

$$q_{f,0}^*(t) = \frac{1}{w_f} [q_0(t) - q_{m,0}^*(t)(1 - w_f)] \quad (25)$$

NUMERICAL SOLUTIONS

The governing dual-porosity water flow and solute transport equations were solved numerically using the Galerkin finite element method assuming linear basis functions. A detailed description of the numerical solutions is given in the appendix. The mathematical accuracy of the numerical scheme was verified by comparing simulation results with those obtained using numerical models for single porosity systems. While assuming no exchange between the pore systems, the water flow and solute transport schemes of each region of the dual-porosity model were tested separately by means of transient flow simulations involving variably saturated conditions. We further used analytical solutions of the two-region mobile-immobile solute transport model to verify the diffusion component of the solute mass transfer formulation (19) assuming steady state flow.

SIMULATION EXAMPLES AND SENSITIVITY STUDIES

The examples presented below serve to illustrate the performance of the proposed model in simulating various physical nonequilibrium situations during transient flow and transport in a dual-porosity type structured porous medium and to show the sensitivity of the model to selected parameters in the first-order mass transfer term for water. We assumed the application of water at a constant rate of 50 cm/d to a 40-cm-deep dual-porosity medium having an initially uniform pressure head of $h_{f,i} = h_{m,i} = -1000$ cm. Water was allowed to infiltrate exclusively into the fracture pore system, thus assuming that the matrix pore system at the surface is in effect sealed. To ensure accurate answers, simulation results given here were obtained with very small element sizes (as small as 0.1 cm) using an adaptive time-stepping scheme [Kool and van Genuchten, 1991] with initial time steps as small as 10⁻⁷ days.

The hydraulic properties of the fracture and matrix pore systems were described using the analytical functions of van Genuchten [1980] as follows:

$$\theta = \theta_r + (\theta_s - \theta_r)[1 + |\alpha h|^n]^{-m} \quad (26)$$

$$K(S_e) = K_s S_e^l [1 - (1 - S_e^{1/m})^m]^2 \quad (m = 1 - 1/n) \quad (27)$$

where θ_r and θ_s are the residual and saturated water contents, respectively, h is the pressure head, K_s is the hydraulic conductivity at saturation, $S_e = (\theta - \theta_r)/(\theta_s - \theta_r)$ is the effective saturation, and α , n , m , and l are empirical parameters. The hydraulic parameters used for the simulations (Table 1) are essentially the same as those employed for Figure 2, except that smaller values of θ_s and θ_r for the fracture pore system were used (instead of $\theta_s = 0.75$ and $\theta_r = 0.1$ as used in Figure 2). The hydraulic parameters of the fracture and matrix are indicative of relatively coarse- and fine-textured soils, respectively. We further assume rectangular aggregates ($\beta = 3.0$) with an average matrix block size of 2 cm ($a = 1$ cm). As suggested by Gerke and van Genuchten [1993], the scaling coefficient, γ_w , was set at 0.4, while the apparent hydraulic conductivity K_a of the transfer term was evaluated as $K_a = 0.5[K_a(h_f) + K_a(h_m)]$. The hydraulic parameters for $K_a(\bar{h})$ were assumed to be the same as those for $K_m(h_m)$, except for the saturated hydraulic conductivity which was decreased by a factor of 100 (Table 1).

Figure 3 shows simulated pressure head and water content profiles during infiltration in a 40-cm-deep dual-porosity system. The water contents ϑ_i are given in terms of the bulk soil volume, i.e.,

$$\vartheta_f = w_f \theta_f; \quad \vartheta_m = w_m \theta_m = (1 - w_f) \theta_m \quad (28)$$

The dual-porosity model predicts a very rapid increase in the pressure head of the fracture pore system but a relatively slow response of the matrix (Figure 3a). The resulting pressure head gradient between the two pore systems leads to a transfer of water from the fracture into the matrix pore system (Figure 3b), with a concomitant increase in the water contents (Figure 3c) and vertical flow rates in the matrix. Significant pressure head differences between the two pore systems can still be observed after $t = 0.08$ days when the infiltration front in the fracture system approaches the bottom of the soil profile (Figure 3a). The water transfer rate Γ_w is highest close to the infiltration front and gradually decreases toward the top of the profile (Figure 3b). The shapes of the curves reflect the net effects on Γ_w of the pressure head differences between the two pore regions, which decrease in time, and the values of K_a , which increase with time, at any particular depth behind the moisture front. The total water transfer rate as integrated over the entire profile was found to remain fairly constant between $t = 0.01$ and $t = 0.08$ days. This feature is shown in Figure 5 which will be discussed in more detail below. At later times, the highest transfer rates occurred at the top of the profile because of increased gravity-dominated vertical flow of water in the matrix pore system (results not further shown here).

The sensitivity of the infiltration process to changes in the matrix block size a is shown in Figure 4 after 0.02 days, again using the parameters listed in Table 1. Simulation

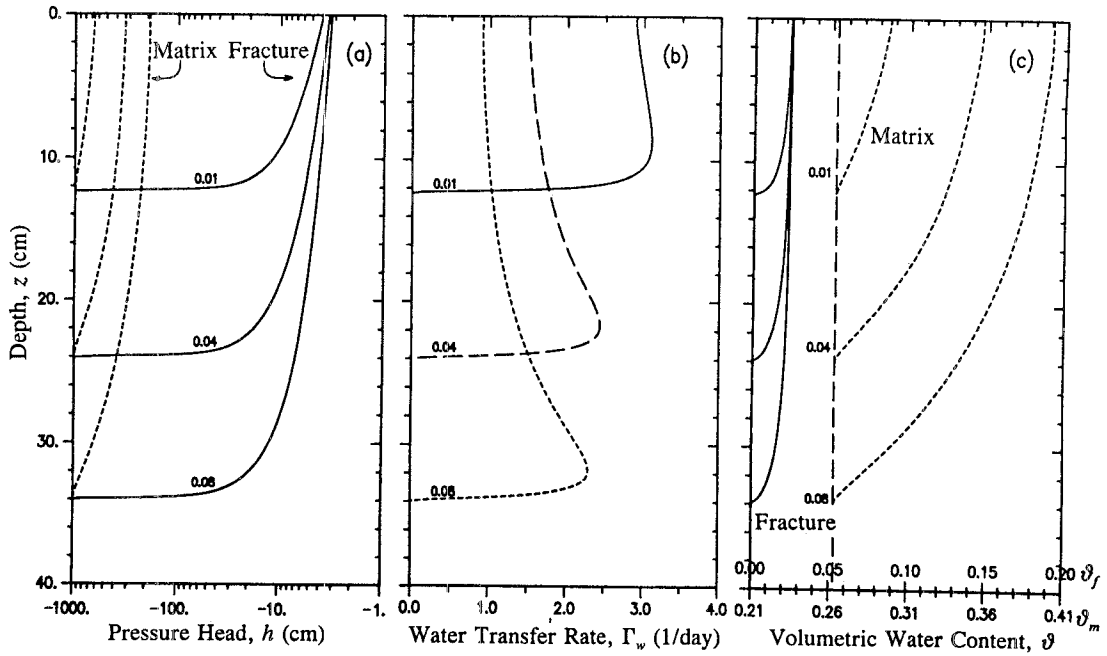


Fig. 3. (a) Simulated pressure head h and (c) volumetric water content ϑ profiles of the matrix (dotted lines) and fracture (solid lines) pore systems, and (b) calculated water transfer rates Γ_w versus depth at $t = 0.01, 0.04,$ and 0.08 days. The water content ϑ (Figure 3c) is related to the total volume of the porous medium; dashed lines indicate the initial water content.

results obtained with a relatively small matrix block size of $a = 0.1$ cm closely approximate the limiting case of pressure head equilibrium (Figure 4a) with no preferential flow. The equilibrium moisture front (Figure 4c) reached a depth of only 5 cm (at $t = 0.02$ days). Notice that the total water content θ of the porous medium as given by (4) is plotted in Figure 4c. The water transfer rates (Figure 4b) are apparently so high that the system quickly approaches equilibrium when $a = 0.1$ cm. However, for the largest matrix block size

($a = 3.3$ cm), water percolated rapidly downward through the fracture pore system to a depth of 35 cm during the same time period ($t = 0.02$ days or 29 min). This last situation represents an extreme case of preferential flow in which pressure head nonequilibrium is very significant (Figure 4a), and water transfer rates are relatively small with only slight changes in Γ_w along the profile (Figure 4b). All other parameter combinations yielded results which were in between those two extreme cases, indicating various degrees of nonequilibrium.

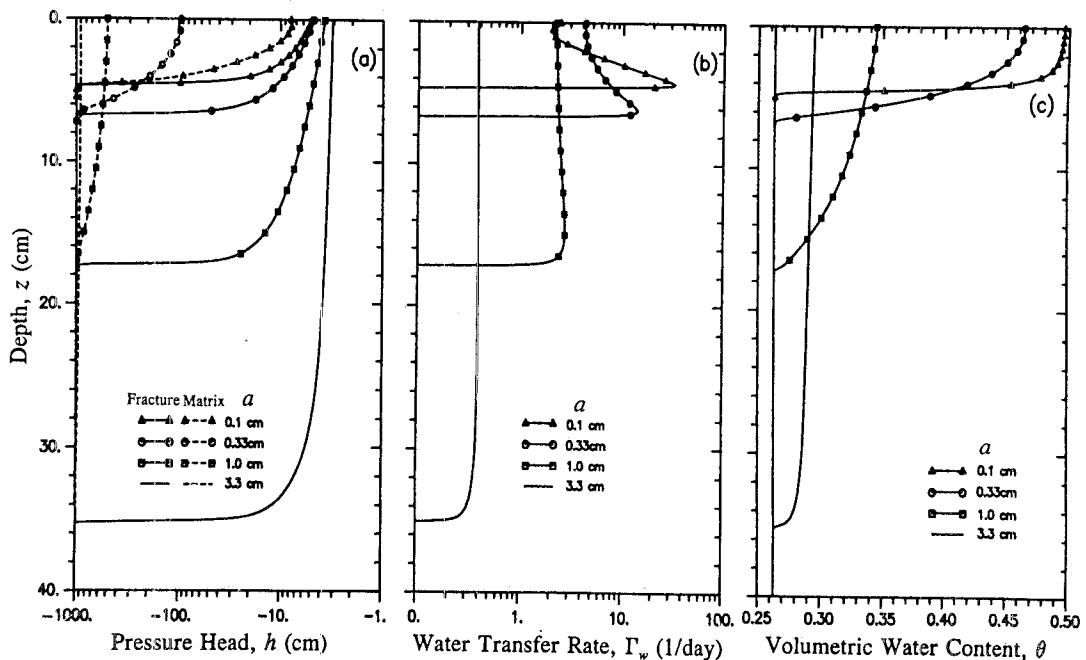


Fig. 4. (a) Simulated pressure head h , (b) water transfer rate Γ_w and (c) total volumetric water content θ versus depth z at $t = 0.02$ days for different matrix block sizes a using $K_{s,a} = 0.01$ cm/d.

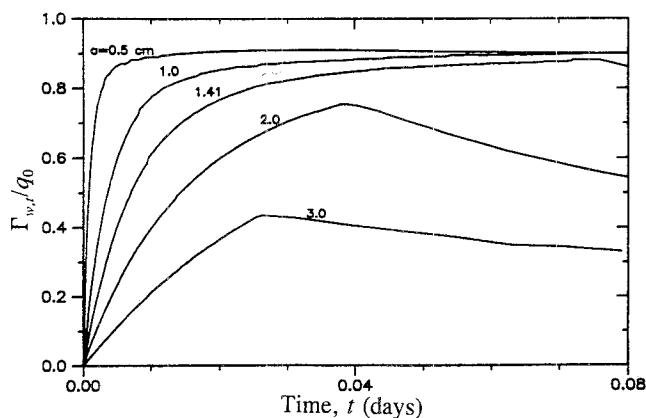


Fig. 5. Ratio between the depth-integrated water transfer rate $\Gamma_{w,t}$ and the infiltration rate q_0 at the soil surface as a function of time for different matrix block sizes a (cm).

The results in Figure 4 were obtained with varying matrix block sizes a and a fixed value of 0.01 cm/d for the effective saturated hydraulic conductivity of the fracture/matrix interface $K_{s,a}$ in the water transfer term. Exactly the same results as in Figure 4 can be obtained by varying $K_{s,a}$ in such a way that for a given value of a the ratios $K_{s,a}/a^2$ remain the same as those in Figure 4. This follows from (15) and (16) which show that the water transfer term α_w is proportional to $K_{s,a}/a^2$. Hence, as expected, a higher value for $K_{s,a}$ leads to faster equilibration between the fracture and matrix pore systems, while a lower $K_{s,a}$ leads to increased preferential flow. The situation where $K_{s,a}$ is equal to the hydraulic conductivity of the matrix $K_{s,m}$ resulted in distributions that were very close to equilibrium (i.e., as those shown by $a = 0.1$ cm in Figure 4).

Figure 5 shows transient changes in the spatially integrated total water transfer rate $\Gamma_{w,t} = \int_0^l \Gamma_w dz$ as a fraction of the infiltration rate q_0 at the soil surface for several matrix block sizes and again assuming a saturated hydraulic conductivity $K_{s,a}$ of 0.01 cm/d. For small values of a , the ratio $\Gamma_{w,t}/q_0$ quickly approaches a fairly constant value of approximately 0.9. This situation represents a quasi-steady-state condition between vertical flow and transfer between the pore systems. Recall that in our example, no water entered the matrix pore system from the top of the profile. Higher values of a require more time before equilibrium is reached. The drop in the ratio when $a \geq 2$ cm (Figure 5) occurs when the moisture front in the fracture system reaches the bottom of the profile. In this case, the depth across which water transfer takes place does not further increase, whereas the pressure differences between the two pore regions still decrease, thus causing lower transfer rates.

The same physical situation as before was used to also simulate solute transport. For simplicity, adsorption and decay were not considered. The dispersion coefficients D_f and D_m in (17a) and (17b) were both described with standard expressions of the form

$$D = D_0\tau + \lambda|\nu| \quad (29)$$

where $D_0\tau$ is the porous media diffusion coefficient (being the product of the diffusion coefficient in free water and the tortuosity factor τ), λ is the dispersivity, and ν is the average pore water velocity. Equation (29) with $D_0\tau = 0.5$ cm²/d

and $\lambda = 2$ cm was applied to both pore systems. The effective diffusion coefficient D_a was assumed to be 0.05 cm²/d. The infiltration of solute-free water into a structured medium having an initial concentration of 1 (e.g., mg/L) was simulated. Because of the distribution of water among the fracture and matrix, 99.9% of the chemical was initially located in the matrix pore system.

Figure 6 shows the simulated leaching of solutes during transient flow as predicted with the dual-porosity model. As solute-free water infiltrates, the solute concentration in the fracture pore system decreases rapidly (Figure 6a). Water with relatively low solute concentration is subsequently transferred from the fracture into the matrix pore system via the convective part of the mass transfer term (compare the water transfer rates shown in Figure 3b). At the same time, however, solutes have a tendency to diffuse back from the matrix into the fracture pore system because of the large concentration gradients (Figure 6a) which develop between the two pore systems. The total solute transfer rates are mostly negative, indicating a net transfer from the matrix into the fracture pore system (Figure 6b). The solute mass in the matrix pore system ($\vartheta_m c_m$) initially decreases only slightly ($t = 0.01$ days in Figure 6c; note the different scales for the two pore systems) but gradually decreases more rapidly from $t = 0.04$ to $t = 0.08$. At later times, solute concentrations (Figure 6a) increase again in the fracture pore system closely behind the moisture front due to continuing transfer, mixing, and dispersion. The rate of solute mass transfer by convection increases after $t = 0.04$ days at greater depths, whereas the diffusive transfer decreases because of the declining gradients. The net transfer eventually becomes positive ($t = 0.08$ days in Figure 6b) near the infiltration front, thus leading to an increase in the solute mass of the matrix pore system at a depth of approximately 30 cm.

The results in Figure 6 reflect the extremely complex and highly transient nature of transport in a dual-porosity medium involving interactions between vertical convective transport, vertical diffusion/dispersion, and horizontal mass transfer and mixing between the fracture and matrix pore systems by convection and diffusion.

DISCUSSION AND CONCLUSIONS

The proposed dual-porosity model is a deterministic approach designed to simplify the description of water flow and solute transport in a structured porous medium such that the model eventually may find application to practical field problems. The model is able to simulate various degrees of nonequilibrium at the macroscopic level by selecting appropriate model parameters. All model parameters can be related to physical properties of the medium, such as the size a and shape β of matrix blocks, or the hydraulic conductivity K_a of the fracture/matrix interface. The combined flow and transport model permits detailed studies of the complex and highly transient processes of leaching or accumulation of solutes under variably saturated conditions.

The study revealed three critical areas of research which need to be further considered: (1) correct representation of the flow regime in the fracture pore system, (2) formulation of the adopted exchange term (14) for water transfer between the two pore systems, and (3) numerical complexities associated with the extremely sharp moisture and concentration

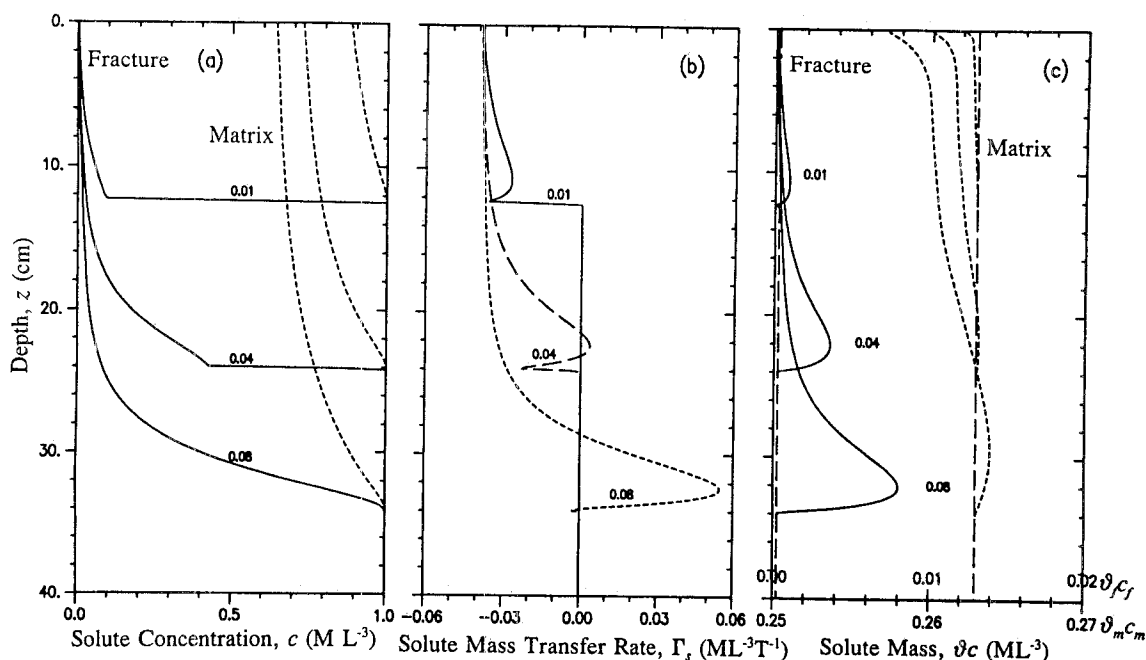


Fig. 6. (a) Simulated solute concentration c and (c) solute mass ∂c profiles of the matrix (dotted curves) and fracture (solid curves) pore systems, and (b) calculated solute transfer rates Γ_s versus depth z at $t = 0.01, 0.04,$ and 0.08 days. The solute mass (∂c) is related to the total volume of the porous medium; dashed lines indicate the initial values; the time (T) unit is days.

fronts in the fracture pore system. These three topics are briefly discussed below.

This study assumed the applicability of the Richards' equation (or Darcy's equation) to variably saturated flow in both pore systems. This assumption may be acceptable for the matrix pore region, but may not be strictly valid for the fracture pore system at relatively high velocities when the flow regime may change from laminar to turbulent. However, an important advantage of also using Richards' equation of the fracture system is the consistency in the description of flow in the two pore systems and the resulting ease of coupling water flow in the two systems. A disadvantage of the current formulation is the highly nonlinear and transient nature of the flow process in the fracture system and the numerical challenges posed by these nonlinearities. Still, the approach gives a consistent, versatile, and integrated process-based description of flow and transport in a structured medium. As such we believe that improvements in predictions resulting from other approximations of the flow regime in the fractures, such as Manning's equation for turbulent overland flow [Chen and Wagenet, 1992a], kinematic wave approaches [e.g., Germann and Beven, 1985], or simple gravity flow models [e.g., Jarvis et al., 1991a], must be meaningful to justify their implementation. This is especially true for field situations where the presence of different flow regimes, initial conditions, and boundary effects combine to yield highly transient flow and transport scenarios which may be exceedingly difficult to describe with the above alternative formulations.

We also note that the advantages of the relatively simple first-order water transfer term proposed here are similar to those of the first-order solute transfer formulation used previously for transport in two-region, mobile-immobile type systems [van Genuchten and Dalton, 1986]. The first-order approach constitutes a significant, yet relatively accurate

simplification which does not require a multidimensional diffusion-based transport model based on a specific geometry of the soil aggregates or rock matrix blocks.

The proposed description introduces a separate hydraulic conductivity function $K_a(h)$ in the transfer coefficient for water in (15). This function is a critical parameter which can significantly affect the rate of water transfer between the matrix blocks and the fracture pore system. Unfortunately, little is known about the physical and chemical properties of the fracture/matrix interface. The few studies known to us (Spengler and Chornack [1984] (as cited by Pruess and Wang [1987]), Gunzelmann [1990] and Thoma et al. [1992]) suggest that the interface hydraulic conductivity can be much less than the conductivity of the matrix interior. This situation would be consistent with our findings that equating K_a with the matrix conductivity K_m will not lead to a significant preferential flow process. The hydraulic conductivities must differ by several orders of magnitude, or the matrix block sizes must be relatively large (Figure 4), in order to allow preferential movement of water over a significant depth. On the other hand, this finding also means that the assumption of pressure head equilibrium between the fracture and matrix pore systems [e.g., Dykhuizen, 1987; Peters and Klavetter, 1988] may well be justified when hydraulic contact between the fracture and the matrix is not restricted. Clearly, some careful experimental studies like those reported by Thoma et al. [1992] are sorely needed.

This study also points to the need for further improvements in numerical solutions of the flow equation when highly nonlinear situations are present. While our numerical solution generally performed well, some problems of stability and lack of mass balance occurred when extremely high local infiltration rates were applied to relatively dry fracture pore systems involving highly nonlinear hydraulic functions. The numerical scheme used for the solute transport model

also tended to produce some minor oscillations at the infiltration front in the fracture pore system where transport was largely dominated by convection. This tendency increased when solute transfer rates between the two pore system increased (large α_s values). More efficient numerical schemes may be especially needed when applying the model to actual field problems. Recent work by Ross [1990] and Ross and Bristow [1991], who applied hyperbolic sine and Kirchhoff transforms to the Richards' equation, by Neuman [1984], who applied a particle tracking method to the advection-dispersion equation, and by Yeh [1990], who used a zoomable hidden fine-mesh system, may prove to be useful for this purpose.

Finally, the application of the dual-porosity model requires estimates of hydraulic, transport, and transfer term parameters which are not easily measured experimentally. Some work has been carried out recently to estimate separated hydraulic parameters for the fracture and matrix pore systems from water retention and hydraulic conductivity measurement on undisturbed soils. Gunzelmann [1990] measured the soil water retention and unsaturated hydraulic conductivity properties of single soil aggregates with microtensimeters. Smettem and Kirby [1990] and Othmer et al. [1991] measured bimodal hydraulic functions of aggregated soils, whereas Durner [1992] and Othmer et al. [1991] derived two-modal and even multimodal retention functions by parameter fitting from experimental data that were obtained using bulk soil samples. While useful, the hydraulic functions must be very well defined in the wet range to accurately approximate the properties of the fracture pore system. This problem is indirectly demonstrated by Figure 2a, which was obtained by assuming that the fracture pore system comprises 5% of the porous medium. In this case, the retention function of the matrix differs only minimally from that of the composite medium. Figure 2a points to the difficulty of clearly distinguishing between separate soil water retention curves of the fracture and matrix pore systems using bulk soil measurements which generally contain some uncertainty. Apart from the retention function, it will be equally challenging to obtain parameters of the transfer terms, as well as the hydraulic properties of the two pore systems for soils containing unstable aggregates, or for soils lacking any visible structure.

Nevertheless, we believe that the proposed model provides a conceptual and numerical framework for studying flow and transport processes in dual-porosity systems using relatively simple parameters which can be related to hydraulic and transport properties of the medium.

APPENDIX: NUMERICAL SOLUTION OF THE DUAL-POROSITY WATER FLOW AND SOLUTE TRANSPORT EQUATIONS

This appendix gives a detailed description of the Galerkin linear finite element schemes used for solving the governing dual-porosity flow and transport equations. Since the Galerkin method has become a relatively standard tool in subsurface flow simulations [e.g., Pinder and Gray, 1977; Huyakorn and Pinder, 1983], only the most pertinent steps in the solution process are given here. Special attention is given to the problem of numerically coupling the flow and transport equations of the two pore regions.

Water Flow Equations

Substituting (14) for Γ_w into (12a) and (12b) using (15), and rearranging leads to the following set of nonlinear partial differential equations with two unknown variables h_f and h_m :

$$L_{w,f}(h_f) \equiv w_f \frac{\partial}{\partial z} \left(K_f \frac{\partial h_f}{\partial z} - K_f \right) - w_f C_f \frac{\partial h_f}{\partial t} - w_f S_f - \alpha_w^* K_a h_f + \alpha_w^* K_a h_m = 0 \quad (A1)$$

$$L_{w,m}(h_m) \equiv w_m \frac{\partial}{\partial z} \left(K_m \frac{\partial h_m}{\partial z} - K_m \right) - w_m C_m \frac{\partial h_m}{\partial t} - w_m S_m + \alpha_w^* K_a h_f - \alpha_w^* K_a h_m = 0 \quad (A2)$$

where $L_{w,f}$ and $L_{w,m}$ are the differential operators for water flow in the fracture and soil matrix regions, respectively, and $w_m = 1 - w_f$. The dependent variables h_f and h_m , are approximated by series \hat{h}_m and \hat{h}_f as follows:

$$h_f(z, t) \approx \hat{h}_f(z, t) = \sum_{j=1}^n \phi_j(z) h_{f,j}(t) \quad (A3)$$

$$h_m(z, t) \approx \hat{h}_m(z, t) = \sum_{j=1}^n \phi_j(z) h_{m,j}(t) \quad (A4)$$

where ϕ_j are piecewise linear basis functions, $h_{m,j}$ and $h_{f,j}$ are the associated time-dependent coefficients representing the solutions of (A1) and (A2) at the finite element nodal points, and n is the total number of nodes. The Galerkin method requires that the differential operators be orthogonal to each of the n basis functions, i.e.,

$$\int_0^l L_{w,f}(\hat{h}) \phi_i(z) dz = 0 \quad i = 1, \dots, n \quad (A5)$$

$$\int_0^l L_{w,m}(\hat{h}) \phi_i(z) dz = 0 \quad (i = 1, \dots, n) \quad (A6)$$

where ϕ_i are the weighing functions which in the Galerkin approach are identical to the basis functions. The integrations in (A5) and (A6) are performed over soil depth l . Substituting (A1) and (A2) into (A4) and (A5), respectively, using integration by parts of the spatial derivatives, and incorporating (A3) and (A4) leads to the matrix equations

$$[A_{f_{ij}}]\{h_{f_j}\} + [B_{f_{ij}}]\{dh_{f_j}/dt\} - [E_{ij}]\{h_{m_j}\} = \{F_{f_j}\} \quad (A7)$$

$$[A_{m_{ij}}]\{h_{m_j}\} + [B_{m_{ij}}]\{dh_{m_j}/dt\} - [E_{ij}]\{h_{f_j}\} = \{F_{m_j}\} \quad (A8)$$

where

$$[A_{f_{ij}}] = w_f \int_0^l K_f \frac{d\phi_i}{dz} \frac{d\phi_j}{dz} dz + \alpha_w^* \int_0^l K_a \phi_i \phi_j dz \quad (A9)$$

$$[A_{m_{ij}}] = w_m \int_0^l K_m \frac{d\phi_i}{dz} \frac{d\phi_j}{dz} dz + \alpha_w^* \int_0^l K_a \phi_i \phi_j dz \quad (A10)$$

$$[B_{f_{ij}}] = w_f \int_0^l C_f \phi_i \phi_j dz \quad (A11)$$

$$[B_{m_{ij}}] = w_m \int_0^l C_m \phi_i \phi_j dz \quad (A12)$$

$$[E_{ij}] = \alpha_w^* \int_0^l K_a \phi_i \phi_j dz \quad (A13)$$

$$\{F_{f_j}\} = -w_f \hat{q}_f \phi_i|_0^l + w_f \int_0^l \left(K_f \frac{d\phi_i}{dz} - S_f \phi_i \right) dz \quad (A14)$$

$$\{F_{m_j}\} = -w_m \hat{q}_m \phi_i|_0^l + w_m \int_0^l \left(K_m \frac{d\phi_i}{dz} - S_m \phi_i \right) dz \quad (A15)$$

in which

$$\hat{q}_f = -\left(K_f \frac{\partial \hat{h}_f}{\partial z} - K_f \right); \quad \hat{q}_m = -\left(K_m \frac{\partial \hat{h}_m}{\partial z} - K_m \right) \quad (A16)$$

Equations (A7) and (A8) together define a set of $m = 2n$ ordinary differential equations with nonlinear coefficients $C_f, C_m, K_f, K_m, K_a, S_f,$ and S_m . These coefficients were expanded over each element in terms of the linear basis functions and the nodal values of the coefficients. The time derivatives in the matrix equation were approximated with fully implicit finite difference schemes. Defining the matrix equations themselves at the half-time level ($t + 1/2\Delta t$) now yields

$$\begin{aligned} & \left([A_f]^{k+1/2} + \frac{1}{\Delta t} [B_f]^{k+1/2} \right) \{h_f\}^{k+1} - [E]^{k+1/2} \{h_m\}^{k+1} \\ & = \frac{1}{\Delta t} [B_f]^{k+1/2} \{h_f\}^k + \{F_f\}^{k+1/2} \end{aligned} \quad (A17)$$

$$\begin{aligned} & \left([A_m]^{k+1/2} + \frac{1}{\Delta t} [B_m]^{k+1/2} \right) \{h_m\}^{k+1} - [E]^{k+1/2} \{h_f\}^{k+1} \\ & = \frac{1}{\Delta t} [B_m]^{k+1/2} \{h_m\}^k + \{F_m\}^{k+1/2} \end{aligned} \quad (A18)$$

where k denotes the time level and Δt is the time step. We further applied mass lumping to the water capacity matrices $[B_f]$ and $[B_m]$ of (A11) and (A12) according to the ‘‘L1 scheme’’ of Milly [1985]. Equations (A17) and (A18) may be solved consecutively by applying an iterative scheme to estimate and update the unknown pressure head vector of the second pore system. Preliminary tests showed that more stable solutions resulted when the equations were solved simultaneously. Therefore (A17) and (A18) were combined to yield a single matrix equation in $2n$ unknowns:

$$[P_{ij}]^{k+1/2} \{h_j\}^{k+1} = \{G_j\} \quad (A19)$$

where $[P]$ is a symmetric seven-diagonal matrix, while h_j comprises both $h_{f,j}$ and $h_{m,j}$. For an arbitrary j th node ($j = 2, \dots, n - 1$), (A19) yields two equations as follows:

$$\begin{aligned} & b_{f_{j-1}} h_{f_{j-1}}^{k+1} + c_{j-1} h_{m_{j-1}}^{k+1} + d_f h_{f_j}^{k+1} \\ & + a_j h_{m_j}^{k+1} + b_f h_{f_{j+1}}^{k+1} + c_j h_{m_{j+1}}^{k+1} = g_{f_j} \end{aligned} \quad (A20)$$

$$\begin{aligned} & c_{j-1} h_{f_{j-1}}^{k+1} + b_{m_{j-1}} h_{m_{j-1}}^{k+1} + a_j h_{f_j}^{k+1} \\ & + d_m h_{m_j}^{k+1} + c_j h_{f_{j+1}}^{k+1} + b_{m_j} h_{m_{j+1}}^{k+1} = g_{m_j} \end{aligned} \quad (A21)$$

where the coefficients are given by

$$a_j = -\frac{\alpha_w^*}{12} [\Delta z_{j-1} (K_{a_{j-1}} + 3K_a) + \Delta z_j (3K_a + K_{a_{j+1}})] \quad (A22)$$

$$b_{f_{j-1}} = -\frac{w_f}{2\Delta z_{j-1}} (K_{f_{j-1}} + K_{f_j}) + \frac{\alpha_w^*}{12} \Delta z_{j-1} (K_{a_{j-1}} + K_a) \quad (A23)$$

$$b_f = -\frac{w_f}{2\Delta z_j} (K_{f_j} + K_{f_{j+1}}) + \frac{\alpha_w^*}{12} \Delta z_j (K_a + K_{a_{j+1}}) \quad (A24)$$

$$c_{j-1} = -\frac{\alpha_w^*}{12} \Delta z_{j-1} (K_{a_{j-1}} + K_a) \quad (A25)$$

$$c_j = -\frac{\alpha_w^*}{12} \Delta z_j (K_a + K_{a_{j+1}}) \quad (A26)$$

$$\begin{aligned} d_f &= \frac{w_f}{2} \left[\frac{1}{\Delta z_{j-1}} (K_{f_{j-1}} + K_{f_j}) + \frac{1}{\Delta z_j} (K_{f_j} + K_{f_{j+1}}) \right] \\ &+ \frac{w_f}{6\Delta t} [\Delta z_{j-1} (C_{f_{j-1}} + 2C_f) + \Delta z_j (2C_f + C_{f_{j+1}})], \\ &+ \frac{\alpha_w^*}{12} [\Delta z_{j-1} (K_{a_{j-1}} + 3K_a) + \Delta z_j (3K_a + K_{a_{j+1}})] \end{aligned} \quad (A27)$$

$$\begin{aligned} g_{f_j} &= \frac{w_f}{6\Delta t} [\Delta z_{j-1} (C_{f_{j-1}} + 2C_f) + \Delta z_j (2C_f + C_{f_{j+1}})] h_{f_j}^k \\ &+ \frac{w_f}{2} (K_{f_{j-1}} - K_{f_{j+1}}) - \frac{w_f}{6} [\Delta z_{j-1} (S_{f_{j-1}} + 2S_f) \\ &+ \Delta z_j (2S_f + S_{f_{j+1}})] \end{aligned} \quad (A28)$$

The coefficients $b_{m,j-1}, b_{m,j}, d_{m,j},$ and $g_{m,j}$ are the same as $b_{f,j-1}, b_{f,j}, d_{f,j},$ and $g_{f,j}$ above, provided the parameters of the fracture pore system ($w_f, K_f, C_f, S_f, h_f^k$) are replaced by the corresponding parameters of the matrix pore system ($w_m, K_m, C_m, S_m, h_m^k$).

Equation (A19) was solved by Gaussian elimination using LU decomposition and back substitution. The scheme uses the Picard iteration method with underrelaxation as described by Cooley [1983]. Convergence criteria, the adaptive time stepping procedure, and estimation of the pressure head values at the new time levels were similar as those used in the HYDRUS code of Kool and van Genuchten [1991]. The soil water capacity terms were evaluated as proposed by Milly [1985]. In case of very small changes in the nodal pressure head, water capacities were calculated directly

from analytical equations of the soil water capacity functions [Kool and van Genuchten, 1991]. The boundary conditions were implemented in the usual manner.

Solute Transport Equations

The Galerkin method was similarly used to solve the coupled set of equations describing solute transport in the fracture and matrix pore systems. For this purpose, the dependent variables c_f and c_m are approximated by

$$c_f(z, t) \approx \hat{c}_f(z, t) = \sum_{j=1}^n \phi_j(z) c_{f,j}(t) \quad (\text{A29})$$

$$c_m(z, t) \approx \hat{c}_m(z, t) = \sum_{j=1}^n \phi_j(z) c_{m,j}(t) \quad (\text{A30})$$

where $\hat{c}_f(z, t)$ and $\hat{c}_m(z, t)$ are the approximate solutions of the solute concentrations in the fracture and matrix pore system, respectively. To solve for the time-dependent coefficients $c_{f,j}$ and $c_{m,j}$, we applied centered-in-time, Crank-Nicholson-type finite difference schemes to the time derivatives, together with dispersion corrections, as explained by van Genuchten [1978]. Equations (17a) and (17b), using (19), and rearranged in terms of the dependent variables, become

$$\begin{aligned} L_s(c_f) \equiv & \frac{w_f}{\Delta t} [(\theta_f R_f c_f)^{k+1} - (\theta_f R_f c_f)^k] \\ & - \frac{1}{2} \left[w_f \frac{\partial}{\partial z} \left(\theta_f D_f^- \frac{\partial c_f}{\partial z} - q_f c_f \right) - t_f c_f - u_m c_m \right]^{k+1} \\ & - \frac{1}{2} \left[w_f \frac{\partial}{\partial z} \left(\theta_f D_f^+ \frac{\partial c_f}{\partial z} - q_f c_f \right) - t_f c_f - u_m c_m \right]^k = 0 \end{aligned} \quad (\text{A31})$$

$$\begin{aligned} L_s(c_m) \equiv & \frac{w_m}{\Delta t} [(\theta_m R_m c_m)^{k+1} - (\theta_m R_m c_m)^k] \\ & - \frac{1}{2} \left[w_m \frac{\partial}{\partial z} \left(\theta_m D_m^- \frac{\partial c_m}{\partial z} - q_m c_m \right) - t_m c_m + u_f c_f \right]^{k+1} \\ & - \frac{1}{2} \left[w_m \frac{\partial}{\partial z} \left(\theta_m D_m^+ \frac{\partial c_m}{\partial z} - q_m c_m \right) - t_m c_m + u_f c_f \right]^k = 0 \end{aligned} \quad (\text{A32})$$

where

$$t_f = w_f \theta_f \mu_f + u_f; \quad t_m = w_m \theta_m \mu_m - u_m \quad (\text{A33})$$

$$u_f = (1-d)\Gamma_w \phi_f + \alpha_s w_m \theta_m \quad (\text{A34})$$

$$u_m = d\Gamma_w \phi_m - \alpha_s w_m \theta_m$$

and where the dispersion correction factors are defined as [van Genuchten, 1978]

$$D_f^- = D_f - \frac{q_f^2 \Delta t}{6\theta_f^2 R_f}; \quad D_f^+ = D_f + \frac{q_f^2 \Delta t}{6\theta_f^2 R_f} \quad (\text{A35})$$

$$D_m^- = D_m - \frac{q_m^2 \Delta t}{6\theta_m^2 R_m}; \quad D_m^+ = D_m + \frac{q_m^2 \Delta t}{6\theta_m^2 R_m} \quad (\text{A36})$$

The finite element analysis from this point on proceeds along the same lines as before for the flow equations. After substituting (A31) and (A32) into the optimization scheme, partial integration of the spatial derivatives, and using (A29) and (A30), the following set of matrix equations results:

$$\begin{aligned} & \left([A_f^-] + \frac{1}{\Delta t} [B_f] + [T_f] \right)^{k+1} \{c_f\}^{k+1} \\ & + [U_m]^{k+1} \{c_m\}^{k+1} = \left(-[A_f^+] + \frac{1}{\Delta t} [B_f] - [T_f] \right)^k \{c_f\}^k \\ & - [U_m]^k \{c_m\}^k + \{F_f\} \end{aligned} \quad (\text{A37})$$

$$\begin{aligned} & \left([A_m^-] + \frac{1}{\Delta t} [B_m] + [T_m] \right)^{k+1} \{c_m\}^{k+1} \\ & + [U_f]^{k+1} \{c_f\}^{k+1} = \left(-[A_m^+] + \frac{1}{\Delta t} [B_m] - [T_m] \right)^k \{c_m\}^k \\ & - [U_f]^k \{c_f\}^k + \{F_m\} \end{aligned} \quad (\text{A38})$$

where

$$[A_{f_v}^-] = \frac{w_f}{2} \int_0^l \left(\theta_f D_f^- \frac{d\phi_j}{dz} - q_f \phi_j \right) \frac{d\phi_i}{dz} dz \quad (\text{A39})$$

$$[A_{f_v}^+] = \frac{w_f}{2} \int_0^l \left(\theta_f D_f^+ \frac{d\phi_j}{dz} - q_f \phi_j \right) \frac{d\phi_i}{dz} dz \quad (\text{A40})$$

$$[B_{f_v}] = w_f \int_0^l \theta_f R_f \phi_i \phi_j dz \quad (\text{A41})$$

$$[T_{f_v}] = \frac{1}{2} \int_0^l t_f \phi_i \phi_j dz \quad (\text{A42})$$

$$[U_{f_v}] = \frac{1}{2} \int_0^l u_f \phi_i \phi_j dz \quad (\text{A43})$$

$$\{F_{f_v}\} = \frac{1}{2} (q_f^{s,k+1} + q_f^{s,k}) \phi_{i|0} \quad (\text{A44})$$

in which

$$q_f^s = \theta_f D_f^- \frac{d\hat{c}_f}{dz} - q_f \hat{c}_f \quad (\text{A45})$$

and where $[A_m^-]$, $[A_m^+]$, $[B_m]$, $[T_m]$, $[E_m]$, and $\{F_m\}$ are the corresponding matrices and vectors containing variables and coefficients with properties of the matrix pore system (θ_m , D_m^- , D_m^+ , q_m , q_m^s , R_m , t_m , u_m , w_m , and \hat{c}_m). To limit numerical oscillations, mass lumping was applied to the time derivatives in equations (A37) and (A38). All coefficients in

(A39)–(A44) were expanded for each element in terms of the linear basis functions.

The element matrices were combined into global matrices for each pore system. The global matrices, in turn, were combined to yield the following single matrix equation containing the unknown concentrations of both pore systems:

$$[P_{ij}^s]^{k+1} \{c_j\}^{k+1} = [Q_{ij}^s]^{k+1} \{c_j\}^k + \{F_j^s\} = \{G_j^s\} \quad (A46)$$

in which $[P^s]$ and $[Q^s]$ are nonsymmetric seven-row diagonal matrices ($i = 1, \dots, 7$). For an arbitrary j th node ($j = 2, \dots, n - 1$) the linear finite element scheme gives

$$a_2^f c_{f_{j-1}}^{k+1} + a_3^m c_{m_{j-1}}^{k+1} + a_4^f c_{f_j}^{k+1} + a_5^m c_{m_j}^{k+1} + a_6^f c_{f_{j+1}}^{k+1} + a_7^m c_{m_{j+1}}^{k+1} = g_{f_j}^s \quad (A47)$$

$$a_1^f c_{f_{j-1}}^{k+1} + a_2^m c_{m_{j-1}}^{k+1} + a_3^f c_{f_j}^{k+1} + a_4^m c_{m_j}^{k+1} + a_5^f c_{f_{j+1}}^{k+1} + a_6^m c_{m_{j+1}}^{k+1} = g_{m_j}^s \quad (A48)$$

where

$$a_1^f = -\frac{\Delta z_{j-1}}{24} (u_{f_{j-1}} + u_j) \quad (A49)$$

$$a_2^f = \frac{-w_f}{4\Delta z_{j-1}} (\theta_{f_{j-1}} D_{f_{j-1}}^- + \theta_f D_{f_j}^-) - \frac{1}{12} (2q_{f_{j-1}} + q_{f_j}) + \frac{\Delta z_{j-1}}{24} (t_{f_{j-1}} + t_f) \quad (A50)$$

$$a_3^f = -\frac{1}{24} [\Delta z_{j-1} (u_{f_{j-1}} + 3u_f) + \Delta z_j (3u_f + u_{f_{j+1}})] \quad (A51)$$

$$a_4^f = \frac{w_f}{4} \left[\frac{1}{\Delta z_{j-1}} (\theta_{f_{j-1}} D_{f_{j-1}}^- + \theta_f D_{f_j}^-) + \frac{1}{\Delta z_j} (\theta_f D_{f_j}^- + \theta_{f_{j+1}} D_{f_{j+1}}^-) \right] + \frac{1}{12} (q_{f_{j+1}} - q_{f_{j-1}}) + \frac{w_f}{6\Delta t} \cdot [\Delta z_{j-1} (\theta_{f_{j-1}} R_{f_{j-1}} + 2\theta_f R_{f_j}) + \Delta z_j (2\theta_f R_{f_j} + \theta_{f_{j+1}} R_{f_{j+1}})] + \frac{1}{24} [\Delta z_{j-1} (t_{f_{j-1}} + 3t_f) + \Delta z_j (3t_f + t_{f_{j+1}})] \quad (A52)$$

$$a_5^f = -\frac{\Delta z_j}{24} (u_f + u_{f_{j+1}}) \quad (A53)$$

$$a_6^f = \frac{-w_f}{4\Delta z_j} (\theta_f D_{f_j}^- + \theta_{f_{j+1}} D_{f_{j+1}}^-) + \frac{1}{12} (q_{f_j} + 2q_{f_{j+1}}) + \frac{\Delta z_j}{24} (t_{f_j} + t_{f_{j+1}}) \quad (A54)$$

and where $a_2^m = a_2^f$, $a_3^m = -a_1^f$, $a_4^m = a_4^f$, $a_5^m = -a_3^f$, $a_6^m = a_6^f$, and $a_7^m = -a_5^f$ provided that in these expressions all parameters of the fracture pore system are replaced by those of the matrix pore system (θ_m , D_m^- , q_m , R_m , t_m , u_m ,

w_m). Vector $\{G^s\}$ combines the elements of matrix $[Q^s]$ and vector $\{F^s\}$. Matrix $[Q^s]$ in (A46) is exactly the same as matrix $[P^s]$, except that D_f^- and D_m^- have to be replaced by $(-D_f^+)$ and $(-D_m^+)$, q_f and q_m by $(-q_f)$ and $(-q_m)$, u_f and u_m by $(-u_f)$ and $(-u_m)$, t_f and t_m by $(-t_f)$ and $(-t_m)$, and w_f by w_m . The entries f_f and f_m of vector $\{F^s\}$ in (A46) are given by

$$f_{f_1} = -\frac{1}{2} [q_f^s(0, k + 1) + q_f^s(0, k)] \quad (A55)$$

$$f_{m_1} = -\frac{1}{2} [q_m^s(0, k + 1) + q_m^s(0, k)] \quad (A56)$$

$$f_{f_j} = 0; \quad f_{m_j} = 0 \quad (j = 2, \dots, n - 1) \quad (A57)$$

$$f_{f_n} = \frac{1}{2} [q_f^s(l, k + 1) + q_f^s(l, k)] \quad (A58)$$

$$f_{m_n} = \frac{1}{2} [q_m^s(l, k + 1) + q_m^s(l, k)] \quad (A59)$$

The solute transport boundary conditions were implemented in the standard way.

REFERENCES

Arbogast, T., J. Douglas, Jr., and U. Hornung, Derivation of the double porosity model of single phase flow via homogenization theory, *SIAM J. Math. Anal.*, 21, 823–836, 1990.
 Baker, R. S., and D. Hillel, Observations of fingering behavior during infiltration into layered soils, in *Preferential Flow*, edited by T. I. Gish and A. Shirmohammadi, pp. 87–99, American Society of Agricultural Engineers, St. Joseph, Mich., 1991.
 Barenblatt, G. I., Iu. P. Zheltov, and I. N. Kochina, Basic concepts in the theory of seepage of homogeneous liquids in fissured rocks, *J. Appl. Math. Mech.*, 24, 1286–1303, 1960.
 Berkowitz, B., J. Bear, and C. Braester, Continuum models for contaminant transport in fractured porous formations, *Water Resour. Res.*, 24, 1225–1236, 1988.
 Beven, K. J., Kinematic subsurface stormflow, *Water Resour. Res.*, 17, 1419–1424, 1981.
 Beven, K. J., On subsurface stormflow: Predictions with simple kinematic theory for saturated and unsaturated flows, *Water Resour. Res.*, 18, 1627–1633, 1982.
 Beven, K. J., Modeling preferential flow: An uncertain future?, in *Preferential Flow*, edited by T. J. Gish and A. Shirmohammadi, pp. 1–11, American Society of Agricultural Engineers, St. Joseph, Mich., 1991.
 Beven, K. J., and P. Germann, Water flow in soil macropores, II, A combined flow model, *J. Soil Sci.*, 32, 15–29, 1981.
 Beven, K. J., and P. Germann, Macropores and water flow in soils, *Water Resour. Res.*, 18, 1311–1325, 1982.
 Bibby, R., Mass transport of solutes in dual-porosity media, *Water Resour. Res.*, 17, 1075–1081, 1981.
 Bolt, G. H., Movement of solutes in soil: Principles of adsorption/exchange chromatography, in: *Soil Chemistry, B. Physico-Chemical Models, Dev. Soil Sci.*, vol. 5B, edited by G. H. Bolt, pp. 295–348, Elsevier, New York, 1979.
 Bond, W. J., and P. J. Wierenga, Immobile water during solute transport in unsaturated sand columns, *Water Resour. Res.*, 26, 2475–2481, 1990.
 Bruggeman, A. C., and S. Mostaghimi, Simulation of preferential flow and solute transport using an efficient finite element model, in *Preferential Flow*, edited by T. J. Gish and A. Shirmohammadi, pp. 244–255, American Society of Agricultural Engineers, St. Joseph, Mich., 1991.
 Brusseau, M. L., and P. S. C. Rao, Modeling solute transport in structured soils: A review, *Geoderma*, 46, 169–192, 1990.
 Chen, C., and R. J. Wagenet, Simulation of water and chemicals in macropore soils, I, Representation of the equivalent macropore influence and its effect on soil-water flow, *J. Hydrol.*, 130, 105–126, 1992a.
 Chen, C., and R. J. Wagenet, Simulation of water and chemicals in

- macropore soils, II, Application of linear filter theory, *J. Hydrol.*, *130*, 127–149, 1992b.
- Coats, K. H., and B. D. Smith, Dead-end pore volume and dispersion in porous media, *Soc. Pet. Eng. J.*, *4*, 73–84, 1964.
- Cooley, R. L., Some new procedures for numerical solution of variably saturated flow problems, *Water Resour. Res.*, *19*, 1271–1285, 1983.
- Davidson, M. R., Numerical calculation of saturated-unsaturated infiltration in a cracked soil, *Water Resour. Res.*, *21*, 709–714, 1985.
- Dudley, A. L., R. R. Peters, J. H. Gauthier, M. L. Wilson, M. S. Tierney, and E. A. Klavetter, Yucca Mountain Project, Total system performance assessment code (TOSPAC), vol. 1, Physical and mathematical bases, *Sandia Rep. Sand85-0002*, Sandia Natl. Lab., Albuquerque, N. M., 1988.
- Duguid, J. O., and P. C. Y. Lee, Flow in fractured porous media, *Water Resour. Res.*, *13*, 558–566, 1977.
- Durner, W., Predicting the unsaturated hydraulic conductivity using multi-porosity water retention curves, in *Indirect Methods for Estimating the Hydraulic Properties of Unsaturated Soils*, edited by M. T. van Genuchten, F. J. Leij, and L. J. Lund, pp. 185–202, University of California, Riverside, 1992.
- Dykhuizen, R. C., Transport of solutes through unsaturated fractured media, *Water Research*, *21*, 1531–1539, 1987.
- Edwards, W. M., R. R. van der Ploeg, and W. Ehlers, A numerical study of the effects of non-capillary size pores upon infiltration, *Soil Sci. Soc. Am. J.*, *43*, 851–856, 1979.
- Evans, D. D., and T. J. Nicholson, Flow and transport through unsaturated fractured rock: An overview, in *Flow and Transport Through Unsaturated Fractured Rock*, *Geophys. Monogr. Ser.* vol. 42, edited by D. D. Evans and T. J. Nicholson, pp. 1–10, AGU, Washington, D. C., 1987.
- Gerke, H. H., and M. T. van Genuchten, Evaluation of a first-order water transfer term for variably saturated dual-porosity flow models, *Water Resour. Res.*, in press, 1993.
- Germann, P., Preferential flow and generation of runoff, 1, Boundary layer flow theory, *Water Resour. Res.*, *26*, 3055–3063, 1990.
- Germann, P., and K. J. Beven, Kinematic wave approximation to infiltration into soils with sorbing macropores, *Water Resour. Res.*, *21*, 990–996, 1985.
- Glass, R. J., T. S. Steenhuis, and J.-Y. Parlange, Mechanism for finger persistence in homogeneous, unsaturated, porous media: Theory and verification, *Soil Sci.*, *148*(1), 60–70, 1989.
- Gunzelmann, M., Quantification and simulation of the water balance of single aggregates and structured total soils with special regard to the water retention/hydraulic conductivity function of single aggregates (in German), Ph.D. thesis, 163 pp., Univ. of Bayreuth, Germany, 1990.
- Gvirtzman, H., M. Magaritz, J. Kanfi, and I. Carmi, Matrix and fissure water movement through unsaturated calcareous sandstone, *Transport Porous Media*, *3*, 343–356, 1988.
- Gvirtzman, H., M. Magaritz, and A. Nadler, Dual water flow pattern in the unsaturated zone under a gypsum-amended soil, *J. Soil Sci.*, *41*, 177–187, 1990.
- Hill, D. E., and J.-Y. Parlange, Wetting front instability in layered soils, *Soil Sci. Soc. Am. Proc.*, *36*, 697–702, 1972.
- Hoogmoed, W. B., and G. F. Bouman, A simulation model for predicting infiltration into cracked clay soil, *Soil Sci. Soc. Am. J.*, *44*, 458–461, 1980.
- Hornberger, G. M., K. J. Beven, and P. Germann, Inferences about solute transport in macroporous forest soils from time series models, *Geoderma*, *46*, 249–262, 1990.
- Hornung, U., and R. E. Showalter, Diffusion models for fractured media, *J. Math. Anal. Appl.*, *147*, 69–80, 1990.
- Huyakorn, P. S., and G. F. Pinder, *Computational Methods in Subsurface Flow*, Academic, San Diego, Calif., 1983.
- Jardine, P. M., G. V. Wilson, and R. J. Luxmoore, Unsaturated solute transport through a forest soil during rain storm events, *Geoderma*, *46*, 103–118, 1990.
- Jarvis, N. J., P.-E. Jansson, P. E. Dik, and I. Messing, Modelling water and solute transport in macroporous soils, I, Model description and sensitivity analysis, *J. Soil Sci.*, *42*, 59–70, 1991a.
- Jarvis, N. J., L. Bergström, and P. E. Dik, Modelling water and solute transport in macroporous soil, II, Chloride breakthrough under non-steady flow, *J. Soil Sci.*, *42*, 71–81, 1991b.
- Kluitenberg, G. J., and R. Horton, Effect of solute application method on preferential transport of solutes in soil, *Geoderma*, *46*, 283–297, 1990.
- Kool, J. B., and M. T. van Genuchten, HYDRUS, One-dimensional variably saturated flow and transport model, including hysteresis and root water uptake, *Res. Rep. 124*, U.S. Salinity Lab., U.S. Dep. of Agric., Agric. Res. Serv., Riverside, Calif., 1991.
- Kung, K.-J. S., Preferential flow in a sandy vadose zone, 1, Field observation, *Geoderma*, *46*, 51–58, 1990a.
- Kung, K.-J. S., Preferential flow in a sandy vadose zone, 2, Mechanisms and implications, *Geoderma*, *46*, 59–71, 1990b.
- Long, J. C. S., J. S. Remer, C. R. Wilson, and P. A. Witherspoon, Porous media equivalents for networks of discontinuous fractures, *Water Resour. Res.*, *18*, 645–658, 1982.
- Luxmoore, R. J., P. M. Jardine, G. V. Wilson, J. R. Jones, and L. W. Zelazny, Physical and chemical controls of preferred path flow through a forested hillslope, *Geoderma*, *46*, 139–154, 1990.
- Milly, P. C. D., A mass-conservative procedure for time stepping in models of unsaturated flow, *Adv. Water Resour.*, *8*, 32–36, 1985.
- Moench, A. F., Double-porosity models for a fissured groundwater reservoir with fracture skin, *Water Resour. Res.*, *20*, 831–846, 1984.
- Neretnieks, I., and A. Rasmuson, An approach to modelling radionuclide migration in a medium with strongly varying velocity and block sizes along the flow path, *Water Resour. Res.*, *20*, 1823–1836, 1984.
- Neuman, S. P., Adaptive Eulerian-Lagrangian finite element method for advection-dispersion, *Int. J. Numer. Methods Eng.*, *20*, 321–337, 1984.
- Nielsen, D. R., M. T. van Genuchten, and J. W. Biggar, Water flow and solute transport processes in the unsaturated zone, *Water Resour. Res.*, *22*, 89S–108S, 1986.
- Othmer, H., B. Dieckrüger, and M. Kutilek, Bimodal porosity and unsaturated hydraulic conductivity, *Soil Sci.*, *152*(3), 139–150, 1991.
- Peters, R. R., and E. A. Klavetter, A continuum model for water movement in an unsaturated fractured rock mass, *Water Resour. Res.*, *24*, 416–430, 1988.
- Pinder, G. F., and W. G. Gray, *Finite Element Simulation in Surface and Subsurface Hydrology*, Academic, San Diego, Calif., 1977.
- Pruess, K., and J. S. Y. Wang, Numerical modeling of isothermal and non-isothermal flow in unsaturated fractured rock—A review, in *Flow and Transport Through Unsaturated Fractured Rock*, *Geophys. Monogr. Ser.*, vol. 42, edited by D. D. Evans and T. J. Nicholson, pp. 11–22, AGU, Washington, D. C., 1987.
- Pruess, K., J. S. Y. Wang, and Y. W. Tsang, On thermohydrologic conditions near high-level nuclear wastes emplaced in partially saturated fractured tuff, 1, Simulation studies with explicit consideration of fracture effects, *Water Resour. Res.*, *26*, 1235–1248, 1990a.
- Pruess, K., J. S. Y. Wang, and Y. W. Tsang, On thermohydrologic conditions near high-level nuclear wastes emplaced in partially saturated fractured tuff, 2, Effective continuum approximation, *Water Resour. Res.*, *26*, 1249–1261, 1990b.
- Ross, P. J., Efficient numerical methods for infiltration using Richards' equation, *Water Resour. Res.*, *26*, 279–290, 1990.
- Ross, P. J., and K. L. Bristow, Simulating water movement in layered and gradational soils using Kirchhoff transform, *Soil Sci. Soc. Am. J.*, *54*, 1519–1524, 1990.
- Schoeneberger, P., and A. Amoozegar, Directional saturated hydraulic conductivity and macropore morphology of a soil-saprolite sequence, *Geoderma*, *46*, 31–50, 1990.
- Skopp, J., W. R. Gardner, and E. J. Tyler, Miscible displacement in structured soils: Two region model with small interaction, *Soil Sci. Soc. Am. J.*, *45*, 837–842, 1981.
- Smettem, K. R. J., and C. Kirby, Measuring the hydraulic properties of a stable aggregated soil, *J. Hydrol.*, *117*, 1–13, 1990.
- Steenhuis, T. S., and J.-Y. Parlange, Preferential flow in structured and sandy soils, in *Preferential Flow*, pp. 12–21, edited by T. J. Gish and A. Shirmohammadi, American Society of Agricultural Engineers, St. Joseph, Mich., 1991.
- Steenhuis, T. S., J.-Y. Parlange, and M. S. Andreini, A numerical model for preferential solute movement in structured soils, *Geoderma*, *46*, 193–208, 1990.
- Thoma, S. G., D. P. Gallegos, and D. M. Smith, Impact of fracture

- coatings on fracture/matrix flow interactions in unsaturated, porous media, *Water Resour. Res.*, 28, 1357-1367, 1992.
- Tsang, Y. W., and C. F. Tsang, Channel model of flow through fractured media, *Water Resour. Res.*, 23, 467-479, 1987.
- van Genuchten, M. T., Mass transport in saturated-unsaturated media: one-dimensional solutions, *Res. Rep. 78-WR-11*, Water Resour. Program, Dep. of Civ. Eng., Princeton Univ., Princeton, N. J., 1978.
- van Genuchten, M. T., A closed-form equation for predicting the hydraulic conductivity of unsaturated soils, *Soil Sci. Soc. Am. J.*, 44, 892-898, 1980.
- van Genuchten, M. T., and F. N. Dalton, Models for simulating salt movement in aggregated field soils, *Geoderma*, 38, 165-183, 1986.
- van Genuchten, M. T., and P. J. Wierenga, Mass transfer studies in sorbing porous media, I, analytical solutions, *Soil Sci. Soc. Am. J.*, 40, 473-480, 1976.
- Wang, J. S. Y., Flow and transport in fractured rocks, *U.S. Natl. Rep. Int. Union Geod. Geophys. 1987-1990, Rev. Geophys.*, 29, suppl., 254-262, 1991.
- Wang, J. S. Y., and T. N. Narasimhan, Hydrologic mechanisms governing fluid flow in a partially saturated, fractured, porous medium, *Water Resour. Res.*, 21, 1861-1874, 1985.
- Warren, J. E., and P. J. Root, The behavior of naturally fractured reservoirs, *Soc. Petrol. Eng. J.*, 3, 245-255, 1963.
- Wheatcraft, S. W., and J. H. Cushman, Hierarchical approaches to transport in heterogeneous porous media, *U.S. Natl. Rep. Int. Union Geod. Geophys. 1987-1990, Rev. Geophys.*, 29, suppl., 263-269, 1991.
- White, R. E., The influence of macropores on the transport of dissolved and suspended matter through soil, *Adv. Soil Sci.*, 3, 95-120, 1985.
- White, R. E., J. S. Dyson, Z. Gerstl, and B. Yaron, Leaching of herbicides through undisturbed cores of a structured clay soil, *Soil Sci. Soc. Am. J.*, 50, 277-283, 1986a.
- White, R. E., J. S. Dyson, R. A. Haigh, W. A. Jury, and G. Sposito, A transfer function model of solute transport through soil. 2, Illustrative applications, *Water Resour. Res.*, 22, 248-254, 1986b.
- Wilson, G. V., and R. J. Luxmoore, Infiltration, macroporosity, and mesoporosity distributions on two forested watersheds, *Soil Sci. Soc. Am. J.*, 52, 329-335, 1988.
- Wilson, G. V., P. M. Jardine, R. J. Luxmoore, and J. R. Jones, Hydrology of a forested hillslope during storm events, *Geoderma*, 46, 119-138, 1990.
- Workman, S. R., and R. W. Skaggs, PREFLO: A water management model capable of simulating preferential flow, *Trans. ASAE*, 33, 1939-1948, 1990.
- Yeh, G. T., A Lagrangian-Eulerian method with zoomable hidden fine-mesh approach to solving advection-dispersion equations, *Water Resour. Res.*, 26, 1133-1144, 1990.
- Yeh, G. T., and R. J. Luxmoore, Chemical transport in macropore-mesopore media under partially saturated conditions, in *Proceedings of Symposium on Unsaturated Flow and Transport Modeling*, edited by E. M. Arnold, G. W. Gee, and R. W. Nelson, pp. 267-281, Pacific Northwest Laboratory, Richland, Wash., 1982.

H. G. Gerke, Destedter Hauptstrasse 1, D-3302 Cremlingen-Destedt, Germany.

M. T. van Genuchten, U.S. Salinity Laboratory, USDA, ARS, 4500 Glenwood Drive, Riverside, CA 92501.

(Received March 20, 1992;
revised September 16, 1992;
accepted October 2, 1992.)

